ADVANCED THERAPEUTICS
www.advtherap.com

Single-Point Laser Irradiation Photodynamic Therapy: From Selective Plasma Damaging to Cell Death from Within the Tumor

Cristina S. Carrizo, Jaime Fernández de Córdoba, Ana Oña, Gianluca D'Agostino, and Sebastián A. Thompson**

Photodynamic therapy (PDT) is a clinically approved anticancer treatment based on the generation of reactive oxygen species (ROS) when a photosensitizing agent (PS) is irradiated with specific light. Typically, irradiation is performed to cover the entire tumor or treatment area. However, this approach presents some disadvantages, including irradiation of the surrounding normal tissue. Therefore, this study introduces a novel phototherapeutic approach using single-point laser irradiation. With the plasma membrane as the primary organelle target, it is demonstrated that single-point laser irradiation induces plasma membrane damage in cancer cells using two clinically approved fluorescent markers for Glioblastoma: Protoporphyrin IX (PPIX), which localizes to the plasma membrane, and Sodium Fluorescein (NaF), which remains in the extracellular space, contacting the membrane. Single-point laser irradiation in photodynamic therapy induces plasma membrane disruption in both cases, resulting in selective necrotic cancer cell death. Interestingly, this approach induces cell death from within the spheroids, and the cell death gradually extends to the rest of the spheroid, minimizing damage to the surrounding tissue. In conclusion, this study presents a novel approach using focused laser irradiation and clinically approved dyes to induce precise, targeted cell death within the tumor, suggesting potential for theranostic applications in tumor eradication.

1. Introduction

PDT is an anti-cancer treatment that relies on the generation of toxic ROS when a PS is irradiated with specific light.[1–5] Generally, these ROS can induce cell death via apoptosis or necrosis, depending on several variables such as PS concentration and localization, light power, and duration of irradiation.[6,7] With the idea of irradiating the whole tumor, usually the light irradiation is induced to a larger area.[8] This logic methodology is meant to achieve the whole tumor eradication and greater penetration depth that increases with the beam size.[8] However, this irradiation can present some disadvantage such us the irradiation to the surrounded normal tissue or the impossibility of targeting specific subcellular compartments. To bring new capabilities to the field of PDT, in this report we explore the performance of Single Point Laser Photodynamic Therapy (SPL-PDT) targeting, as example, the plasma membrane. As it described in the last years, targeting the plasma membrane have the advantages of lower time of dye incubation and rapid cell death by necrosis.[5,6,9–11] Here, we present the capabilities of SPL-PDT using two clinical fluorescent markers that interestingly remain within or close to the plasma membrane: PPIX (metabolized from 5-Aminolevulinic Acid (5-ALA)) and NaF, respectively.[12] These dyes are employed to visualize Glioblastoma in the operation room. 5-ALA/ PPIX and NaF present a different mechanism by which they localize in the tumor.[13] When 5-ALA is administered to the patient, it is metabolized by the tumor cells into PPIX, the molecule that fluoresces under blue light. This tumor localization is used by neurosurgeons to define the tumor borders. On the other hand, NaF is injected intravenously just before the intervention due to its rapid tumor localization.[12–16] The tumor localization of NaF is based on the vascular leakage present in the tumor compared to normal tissue. While not as specific as 5-ALA, both fluorescent markers are currently employed to guide surgery based on their fluorescent properties. Fluorescence-guided surgery has improved the precision and effectiveness of glioblastoma resection and, thus, patient survival.[17–20]

C. S. Carrizo, S. A. Thompson
Madrid Institute for Advanced Studies in Nanoscience (IMDEA Nanociencia)
Madrid 28049, Spain
E-mail: sebastian.thompson@imdea.org
C. S. Carrizo, S. A. Thompson
Nanobiotechnology Unit Associated to the National Center for Biotechnology (CNB-CSIC-IMDEA)
Calle Faraday, 9, Madrid 28049, Spain
J. Fernández de Córdoba, A. Oña, G. D'Agostino
Advanced Light Microscopy
Centro Nacional de Biotecnología (CNB-CSIC)
Madrid 28049, Spain
E-mail: gdagostino@cnb.csic.es

The ORCID identification number(s) for the author(s) of this article can be found under https://doi.org/10.1002/adtp.202400541

DOI: 10.1002/adtp.202400541

Taking advantage of the dye's localization in the tumor, current research also includes the utilization of these fluorescent markers as PSs in PDT. In this report, we employ these dyes to demonstrate the capability of SPL-PD. We believe that SPL-PDT extend the PDT capability and, after future validations in animal models and clinical samples isolated from tumors, the outcomes of SPL-PDT can rapidly be translated to the clinic since employs clinical fluorescent markers.

2. Experimental Section

2.1. Reagents

Dulbecco's modified Eagle medium (DMEM)–Glutamax (31966 057), penicillin–streptomycin (15070-063), and DMEM without phenol red (21063-029) were purchased from GIBCO. Fetal bovine serum (SV30160.3) from HyClone was heat inactivated at 56 °C for 30 min before use. The dishes for microscope imaging were 35 mm culture dishes with 20 mm treated glass bottom surface (734 2904, VWR).

2.2. Cell Culture Preparation

HELA and U87 cells were maintained in DMEM–Glutamax medium, supplemented with 10 % fetal bovine serum and penicillin–streptomycin, at 37 °C, 5 % CO2 atmosphere. U87 cells were washed in phosphate buffer saline (PBS) solution and detached with 0.05 % trypsin diluted in medium. For the experiments, 35 000 cells were plated on 35 mm culture dishes, in a final volume of 2 mL of growing medium. 24 h after, the medium was replaced by complete medium (Serum 10%) or complete medium. NaF final concentration was 1 μM. Cell were incubated with 5-ALA (1 μM) for 24 h with or without serum.

2.3. Spheroids Culture

U87 cells were detached, counted and centrifuged at 1100 rpm, 5 min at room temperature. Cells were diluted to have a final concentration of 500 cell / 20 μL and were plated drop by drop in the upper lid of a p60 petri dish and were cultured inverted allowing spheroid formation by gravity. In order to avoid evaporation, 1 mL of sterile PBS was added in each dish. Cells were cultured for 72 h under standard culture conditions. Before the experiment, the drops from each dish were carefully collected using complete medium and transferred to a μ-slide 8 well glass bottom dish (IBIDI) for confocal analysis.

2.4. Confocal Microscopy

Cells were plated as described previously in the cell culture preparation paragraph of this material and methods section. Images were acquired using a Leica STELLARIS 8 STED 3X multispectral confocal system (Leica Microsystems) equipped with an incubation system (Okolab) to maintain living cells under standard culture conditions (37 °C, 5 % CO2), and using a water immersion HC PL APO CS2 63x NA 1.20 objective (Leica Microsystems). For fluorescein imaging, samples excitation was achieved using a White laser line (WLL) settled at 488 nm with a power of 101 nW or 405 nW for 2D monolayers or spheroids respectively, measured at the sample plane. Fluorescence emission was collected using a hybrid spectral (HyD S1) detector in the range of 500–672 nm, settled in analog mode with gain factor settled at 38.3% for 2D monolayer experiments or at 9.8% for spheroid experiments. For PPIX imaging, samples excitation was achieved using a 405 nm laser with a power of 1.30 nW measured at the sample plane, and fluorescence emission was collected using a hybrid spectral (HyD S3) detector in the range of 614–755 nm, settled in analog mode with gain factor settled at 41 %. For PI imaging samples excitation was achieved using a White laser line (WLL) settled at 550 nm with a power of 205 nW measured at the sample plane, and fluorescence emission was collected using a hybrid spectral (HyD S3) detector in the range of 614–755 nm, settled in analog mode with gain factor fixed at 2.5%. Transmitted light images were acquired using a Trans PMT and gain settled at 24.1 %, using the same 488 nm laser. For experiments showed in **Figure 1**. 3, 4, 5, and 6, pixel size was 241 nm, and single images focusing the median cell plane have been acquired. For experiments showed in **Figure 2**, pixel size was 180 nm. For spheroids z-stack a Z step size of 1 μm have been used. 3D image reconstruction was performed using the 3D package of the LAS X software. Bleaching conditions for experiments performed in Figures 2 and **3** were achieved using the WLL in the bleach point mode settled at 488 nm (fluorescein) or 580 nm (PPIX) with a power of 4.2 μW or 10.7 μW respectively, measured at the sample plane, for 1 min. U87 cells were irradiated 1 min (Fluorescein) and 30 seoconds (PPIX) while HELA was irradiated for 30 s (Fluorescein) and 15 s (PPIX) For experiments presented in Figure 5 laser spheroids were irradiated using the same laser conditions for 3 min. In order to visualize fluorescein or PI internalization, images were acquired 10 min and 1 h after laser bleaching. Plasma membrane marker (Wheat Germ Agglutinin) was incubated with cells at a concentration of 5–10 μg mL^{-1} for 10–30 min at 37C. Apoptosis was detected using CellEvent Caspase-3/7 Detection Reagents (C10430) following manufacturer's protocol.

3. Results

3.1. Fluorescein and Protoporphyrin Localization in U87 Glioblastoma Cells under Different Serum Conditions

We first evaluated the localization of NaF and PPIX in U87 glioblastoma cells cultured under various serum conditions to cover the different clinical scenarios. As it can be observed in Figure 1a, confocal images revealed the same extracellular pattern of NaF distribution independently on the serum availability. As it is already reported,[15] concerning the intracellular Fluorescein concentration, cells cultured without serum for 24 and 48 h showed progressively increased fluorescence intensity (Figure 1a,b) but insignificant compared with the extracellular NaF concentration. Moreover, we showed that PPIX localizes specifically within the plasma membrane of U87 glioblastoma cells cultured in the absence of serum (Figure 1c,d).

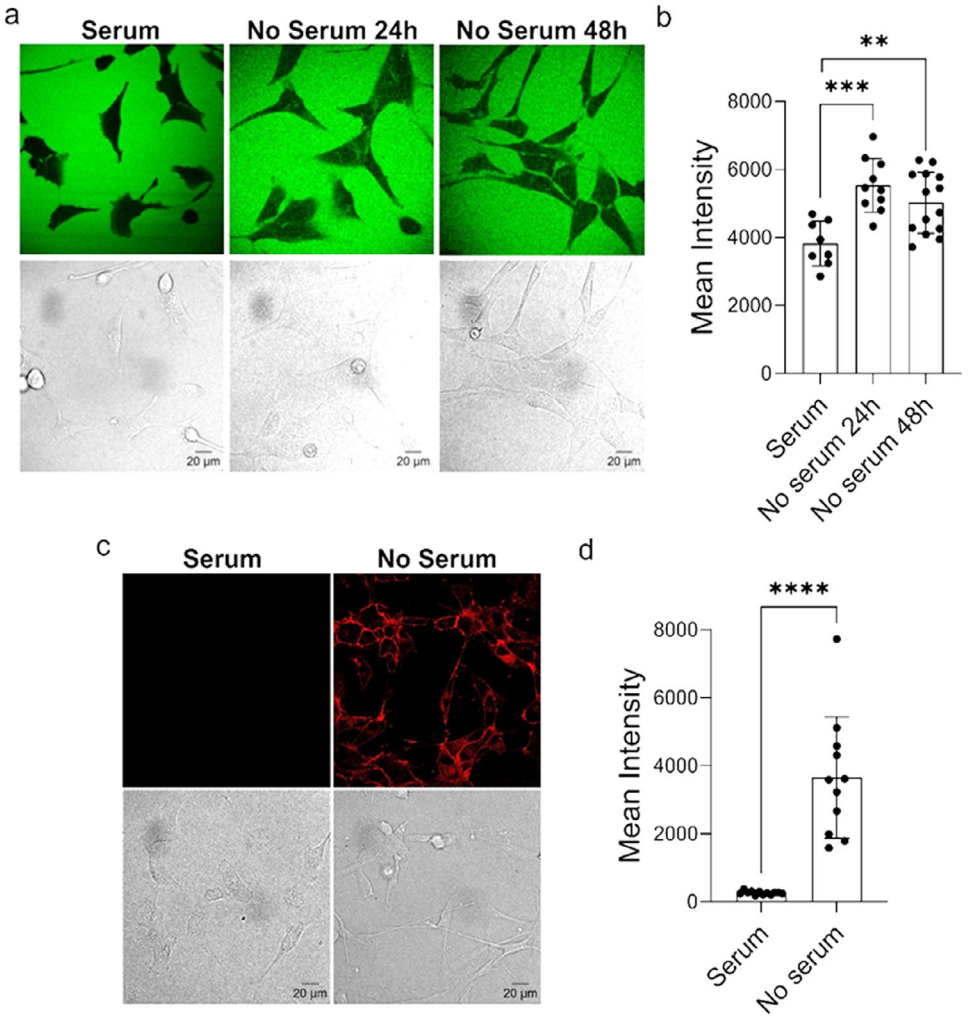

Figure 1. NaF and PPIX cellular localization in U87 glioblastoma cell line. a) Representative confocal images of fluorescein (upper panels) or bright field images (lower panel) of U87 cells cultured with serum (left panel), without serum for 24 h (central panel) or 48 h (right panel). Scale bar is 20 µm. b) Mean fluorescence intensity quantification of fluorescein in cells cultured with serum, or without serum for 24 h or 48 h. ** *P* value = 0.0036, and *** *P* value = 0.0002. c) Representative confocal images of protoporphyrin (upper panels) or bright field images (lower panel) of U87 cells cultured with serum (left panel), or without serum for 24 h (right panel). Scale bar is 20 µm. d) Mean fluorescence intensity quantification of protoporphyrin in cells cultured with serum, or without serum for 24 h. **** *P* value < 0.0001. Concerning PPIX, the localization on the plasma membrane and mitochondria is presented when cells were incubated without serum for 24 h compared to those with serum, as confirmed by confocal imaging and quantitative analysis (Figure 1c,d). These findings agree with the literature where the mechanism involve the transport of the PPIX by the Bovine Serum Albumin (BSA) to the extracellular compartment.

3.2. SPL-PDT Induces Plasma Membrane Damage Following Laser Bleaching in U87 Cells Treated with NaF and PPIX

Since the two fluorescent markers are localized close or on the plasma membrane, we explore the possibility of plasma membrane damage by laser bleaching of U87 cells. The results obtained in 2D Glioblastoma cell culture are shown in Figure 2.

As it can be observed in the Figure 2a–d, the plasma membrane damaging is only observed when the dyes are present. In untreated control cells (Figure 2a–c) laser bleaching did not visibly alter the plasma membrane, as evidenced by the unchanged bright field images. In contrast, cells treated with NaF and exposed to laser bleaching exhibited visible damage to the plasma membrane at the bleaching sites, highlighted by decreased fluorescence intensity and structural disruptions in the irradiated regions (Figure 2b). Concerning PPIX, the same effect is presented in cells treated with protoporphyrin and 5-ALA, where laser irradiation led to clear membrane damage in serum-deprived conditions (Figure 2d). The observed damage was corroborated by magnified images of the irradiated areas, showing marked plasma membrane compromising post-bleaching and the absence of plasma membrane after irradiation only in NaF treated cells. These findings suggest that both fluorescein and protoporphyrin sensitize the plasma membrane to laser-induced damage. Interestingly, PPIX induces greater plasma membrane damage than NaF, as evidenced by the extent of membrane disruption and bubble formation (Figure 2g). Should be noted that the same results were obtained using HELA cells (Figure S1, Supporting

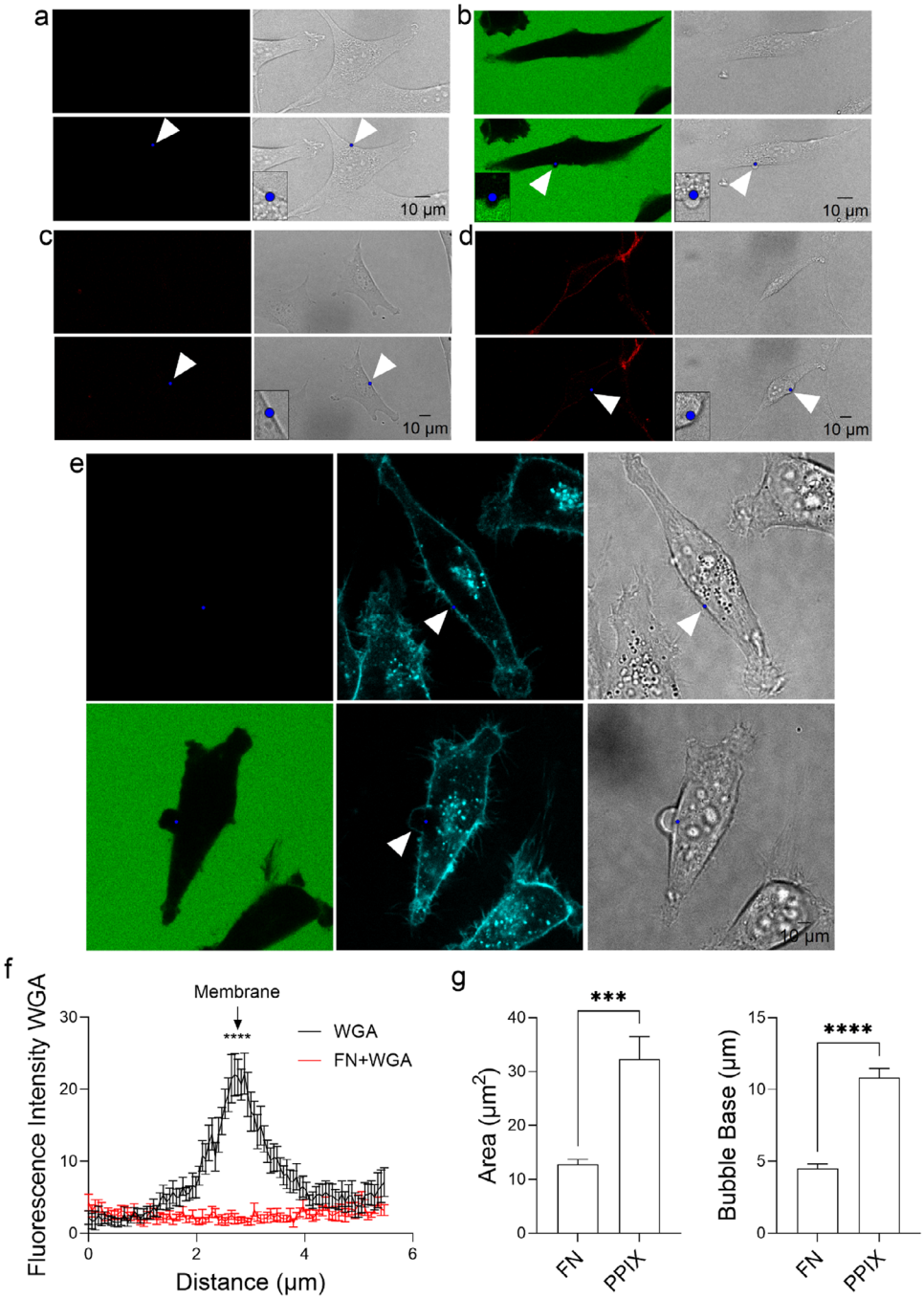

Figure 2. Plasma membrane impairment upon laser bleaching in U87 cells treated with fluorescein and protoporphyrin. a) Representative confocal images of NaF (left panel) or bright field images (right panels) of control U87 cells, untreated with NaF, before bleaching (upper panel) or after bleaching (bottom panel). Bleaching points are highlighted with blue dots and white arrows. Magnified area corresponding to the irradiated plasma membrane region, highlighted by the rectangular selection in the post-bleaching bright field image, is represented (small left panel). Scale bar is 10 µm. b) Representative confocal images of NaF (left panel) or bright field images (right panels) of U87 treated with NaF before bleaching (upper panel) or after bleaching (bottom panel). Bleaching points are highlighted with blue dots and white arrows. Magnified area corresponding to the irradiated plasma membrane region, highlighted by the rectangular selection in the post-bleaching bright field image, is represented (small left panel). Scale bar is 10 µm. c) Representative confocal images of protoporphyrin (left panel) or bright field images (right panels) of control U87 cells, treated with 5-ALA with serum, before bleaching (upper panel) or after bleaching (bottom panel). Bleaching points are highlighted with blue dots and white arrows. Magnified area corresponding to the irradiated plasma membrane region, highlighted by the rectangular selection in the post-bleaching bright field image, is represented (small left panel). Scale bar is 10 µm. d) Representative confocal images of protoporphyrin (left panel) or bright field images (right panels) of U87 cells treated with 5-ALA without serum, before bleaching (upper panel) or after bleaching (bottom panel). Bleaching points are highlighted with blue dots and white arrows. Magnified area corresponding to the irradiated plasma membrane region, highlighted by the rectangular selection in the post-bleaching bright field image, is represented (small left panel). e) Representative confocal images of cells after irradiation: control (top left panel) or treated with

Information). To confirm that the plasma membrane was compromised, we label the plasma membrane with Wheat Germ Agglutinin (WGA-plasma membrane marker). As it can be observed on Figure 2e, the plasma membrane is destroyed (absence of the plasma membrane marker) where the laser was irradiated. This lack of plasma membrane was only presented in PS-treated cells as supported by the quantification of the WGA fluorescence levels within the irradiated region of the plasma membrane which is significantly different between NaF treated cells compared to control counterpart (Figure 2f). Control experiment in Figure 2e (no PS and irradiation) confirm that the plasma membrane marker is not photo bleached. Interestingly, only when the irradiation is performed in a single point, the plasma membrane is compromised and not when the irradiation is performed in a bigger area highlighted by the red rectangular region (Figure S2, Supporting Information).

3.3. SPL-PDT for Plasma Membrane Impairment and Cell Death Induction in U87 Cells

To confirm the plasma membrane is compromised and the damage is not reversible (under these conditions), we follow the irradiated cells through time. Concerning NaF, the confocal images presented in Figure 3a demonstrate the impairment of the plasma membrane and the internalization of the NaF to the intracellular compartment.

This trend was mirrored in protoporphyrin-treated cells but utilizing propidium iodide staining, which indicates compromised membrane integrity and the subsequent induction of cell death.[21] The time-dependent damage captured in the bright field images provides visual evidence that laser-induced bleaching in combination with photosensitizers disrupts cellular structure, ultimately leading to cell death. As it can be noted in both situations, the cell death is only induced to the irradiated cell and not to the surrounding no-irradiated cells, further supporting the specificity of laser bleaching. To identify the cell death mechanism, we studied caspase-3/7 activation, a hallmark of apoptosis. As shown in Figure 3c, caspase-3/7 remains inactive in both FN- and PPIX-treated cells after been irradiated. As a positive control, cells treated with H_2O_2 exhibit caspase-3/7 activation, as indicated by the increased intensity of the apoptosis marker (Figure 3d).

3.4. Localization of Fluorescein and Protoporphyrin in U87 Spheroids

To implement these findings in a clinically relevant model,[22] we first study the localization of the markers in U87 spheroids. **Figure 4** highlights the spatial localization of NaF and protoporphyrin within U87 spheroids. Confocal z-stack images (Figure 4a) showed that fluorescein accumulated primarily in the outer layers of the spheroid, while in the inside some extracellular regions show accumulation of NaF (Figure 4a,c). As it is expected, the PPIX is localized in the same intracellular organelles and in the plasma membrane (Figure 4b,d) corroborating the results described above obtained in 2D monolayer models.

3.5. SPL-PDT in U87 Spheroids

Then, we tested the effects of laser bleaching on U87 spheroids. Concerning the NaF, taking advantage of the dye localized inside the spheroids, the bleaching was performed inside the spheroids to minimize the possible irradiation outside the spheroids (normal tissue). As it can be observed in **Figure 5**a, the structure of the spheroids is compromised as it is illustrated in the time-laps images (Figure 5a).

Bright field images confirmed the physical disruption caused by laser irradiation (Figure 5a second row). 30 min post-bleaching, confocal images revealed a more pronounced entry of fluorescein, indicating that laser treatment not only impairs fluorescence but may also induce structural changes in the spheroid that influence compound retention (Figure 5a-right image). Together with that, the PI internalization was observed in the irradiated zone only in the spheroids treated with NaF (Figure 5b and control-no NaF Figure 5c). Quantification of both Fluorescein and PI internalization are shown in Figure 5d,e showing that SPL-PDT induced NaF internalization (significant after 20 and 30 min upon irradiation) as well as cell death, as suggested by PI accumulation at the irradiation site within the spheroids, only in NaF-irradiated treated spheroids and not in the respective controls not treated with the PS and not irradiated, supporting our previous findings obtained in single cell experiments.

On the other hand, we tested the effects of laser bleaching on PPIX localization within U87 spheroids (Figure 5f). PPIX was initially well-distributed across the spheroid (Figure 5f, upper left panel), and, after irradiation, there was a photobleaching in the region irradiated (Figure 5f, second row). Of note, 10 min after PI addition, the dye only penetrated in the irradiated cells with compromised plasma membranes (Figure 5f, center right panel). By 1-h post-irradiation (Figure 5f right image), the spheroid exhibited widespread cell death, as reflected in the propidium iodide accumulation, demonstrating the efficacy of laser treatment in combination with protoporphyrin for inducing cell death in 3D tumor models (quantification Figure 5g). Notably, representative confocal maximal z-projection of propidium iodide, corresponding to the spheroid, 10 min post laser irradiation (Figure 5h) further demonstrate that laser bleaching was restricted to a single area of the spheroid.

4. Discussion

Here we present a novel photodynamic mechanism based on compromising the plasma membrane by single point laser: SPL-PDT. In the case on damaging the plasma membrane, the localization of the fluorescent marker on or close by the plasma

NaF (bottom left panel). Center panels: cells labeled with a plasma membrane marker. Bleaching points are highlighted with blue dots. Right panels: bright-field images. Scale bar is 10 ϵm f) Quantification of plasma membrane marker intensity comparing control cells (black line) with cells treated with NaF (red line). g) Bubble quantification (bubble size—area—and plasma membrane damage—distance) in cells treated with NaF or PPIX and irradiated under the same conditions.

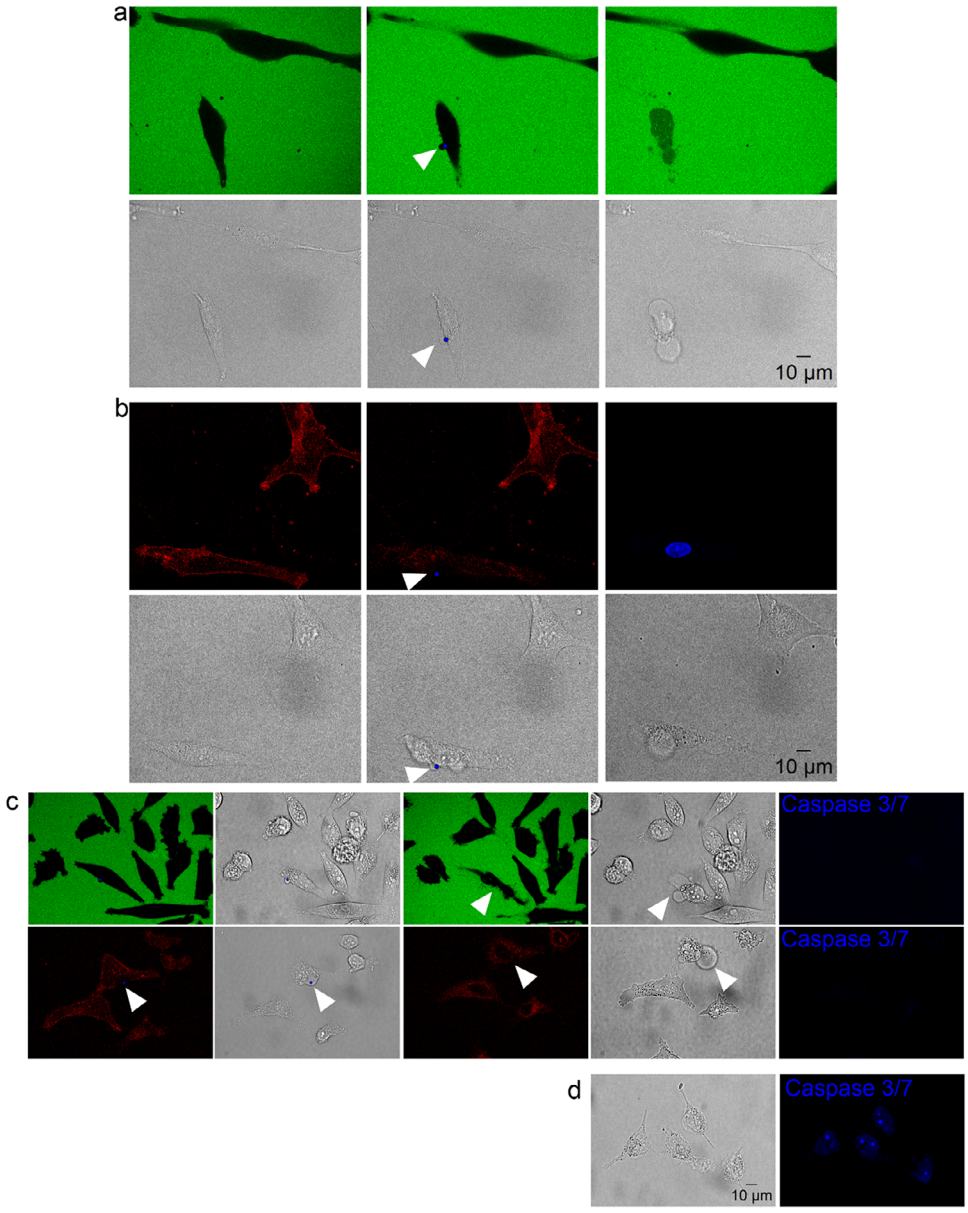

Figure 3. Plasma membrane impairment and cell death induction in U87 cells treated with NaF or protoporphyrin. a) Representative confocal images of fluorescein (upper panel) or bright field images (lower panels) of U87 cells treated with fluorescein before bleaching (left panel), after bleaching (central panel) and 15 min after laser bleaching (left panel). Bleaching points are highlighted with blue dots and white arrows. Scale bar is 10 µm. b) Representative confocal images of protoporphyrin (red-upper panel), propidium iodide (blue-upper right panel) or bright field images (lower panels) of U87 cells treated with fluorescein before bleaching (left panel), after bleaching (central panel) and 15 min after laser bleaching (right panel). Bleaching points are highlighted with blue dots. (c) Representative confocal images of irradiated cells treated with NaF (upper panels) or protoporphyrin (bottom panels), showing no activation of caspase-3/7 (right panels). d) Cells treated with H_2O_2 showing caspase-3/7 activation (positive control). Bleaching points are highlighted with blue dots and white arrows. Scale bar is 10 µm.

membrane is requiered.[5,6,9–11] To achieve this, we first investigated the localization of the clinical markers NaF and PPIX. Concerning NaF, we demonstrated that it remains extracellularly, independent of the serum concentration. This localization is observed in both 2D cell culture and spheroids. Regarding PPIX, consistent with the literature,[23] we observed the porphyrin located in the mitochondria and plasma membrane only in serum-deprived cell culture conditions. When serum is present, it is believed that PPIX is actively extracted by binding to albumin. Once the localization of both markers was defined in 2D cell culture models, we explored the possibility of inducing plasma membrane damage using a point-focused laser. The objective of this damage is to enable selective induction of single-cell death. For this, we induced plasma membrane compromising using both clinical markers. The plasma membrane damage was demonstrated by tracking the uptake of NaF or PI (in the case of PPIX).

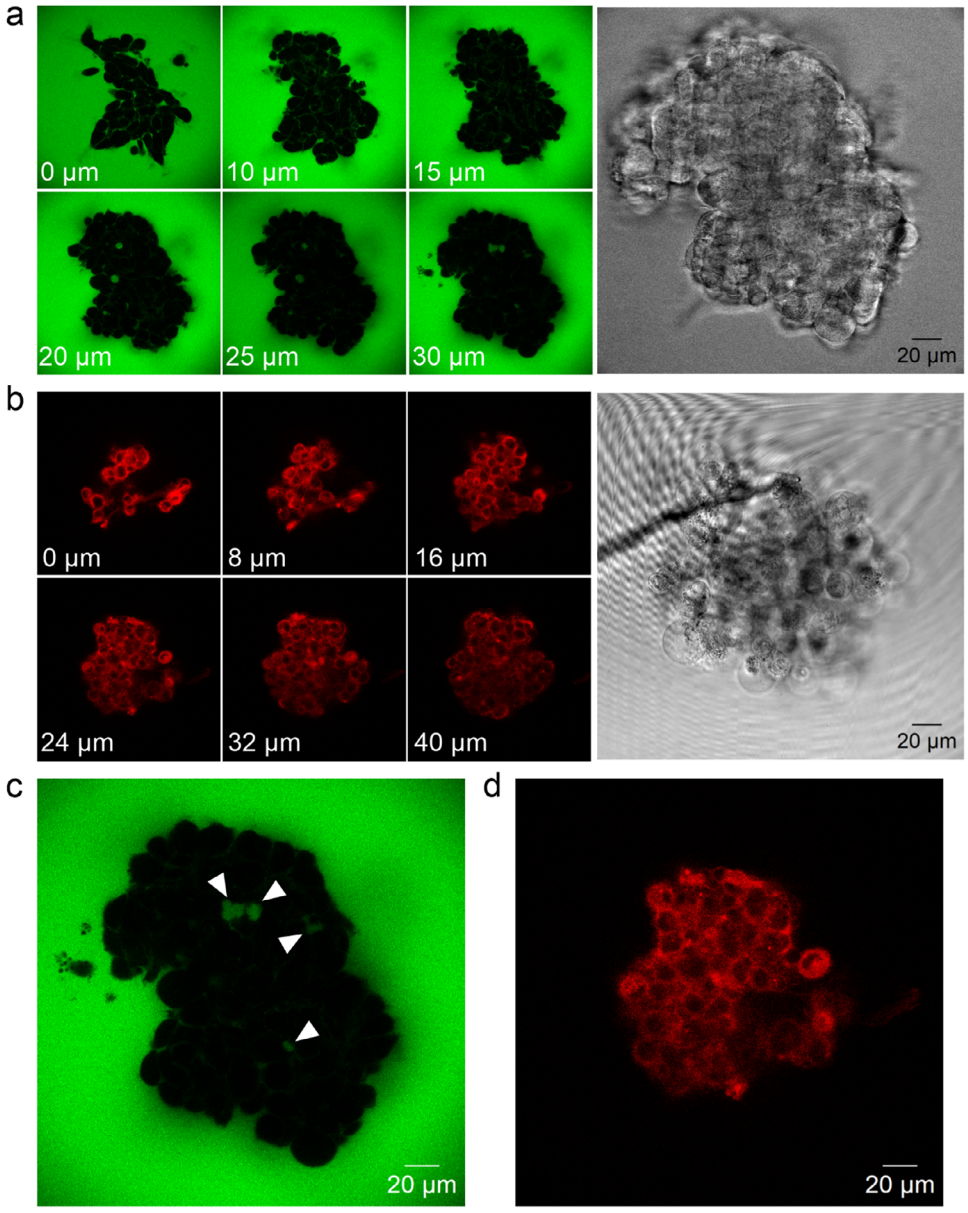

Figure 4. Fluorescein and protoporphyrin localization in U87 spheroids. a) Representative confocal z-stack images of fluorescein (green-left panel) and bright field image (grey-right panel) of a U87 spheroids treated with fluorescein. White labels indicate the z-stack range between images. Scale bar is 20 µm. b) Representative confocal z-stack images of protoporphyrin (red-left panel) and bright field image (grey-right panel) of a U87 spheroids treated with 5-ALA without serum. White labels indicate the z-stack range between images. Scale bar is 20 µm. c) Magnification of the 30 µm image presented in panel a. Scale bar is 20 µm. d) Magnification of the 24 µm image presented in panel b. Scale bar is 20 µm.

As expected, cell death followed plasma membrane compromise based on the damage incurred. We have demonstrated that the plasma membrane is damaged close to the laser irradiation point (Figure 2e). In addition, we have quantified that the plasma membrane damage is bigger in PPIX treated cells compare with fluorescein treated cells (Figure 2g). This is expected since the PPIX is located on the plasma membrane while the fluorescein remains extracellularly (close to the plasma membrane). This damage was only induced when the laser was focused on one point rather than wide-area irradiation (Figure S1b, Supporting Information). Concerning selectivity, it should be noted that this technique is highly selective to only the cell irradiated. As shown in Figure 3, there is no plasma membrane damage induced in the neighboring cells. However, stress can be observed in the surrounding cells due to the cell death induced in the irradiated cell.

The cell death mechanism was also investigated. For this, we employed an apoptosis marker for caspase-3/7 together with propidium iodide (PI) incorporation. As shown in Figure 3c,d, caspase-3/7 was not activated. This, together with PI incorporation, indicates that the main form of cell death is necrosis.

This cell death mechanism was later tested in spheroids. We then evaluated the ability of SPL-PDT to induce cell death in

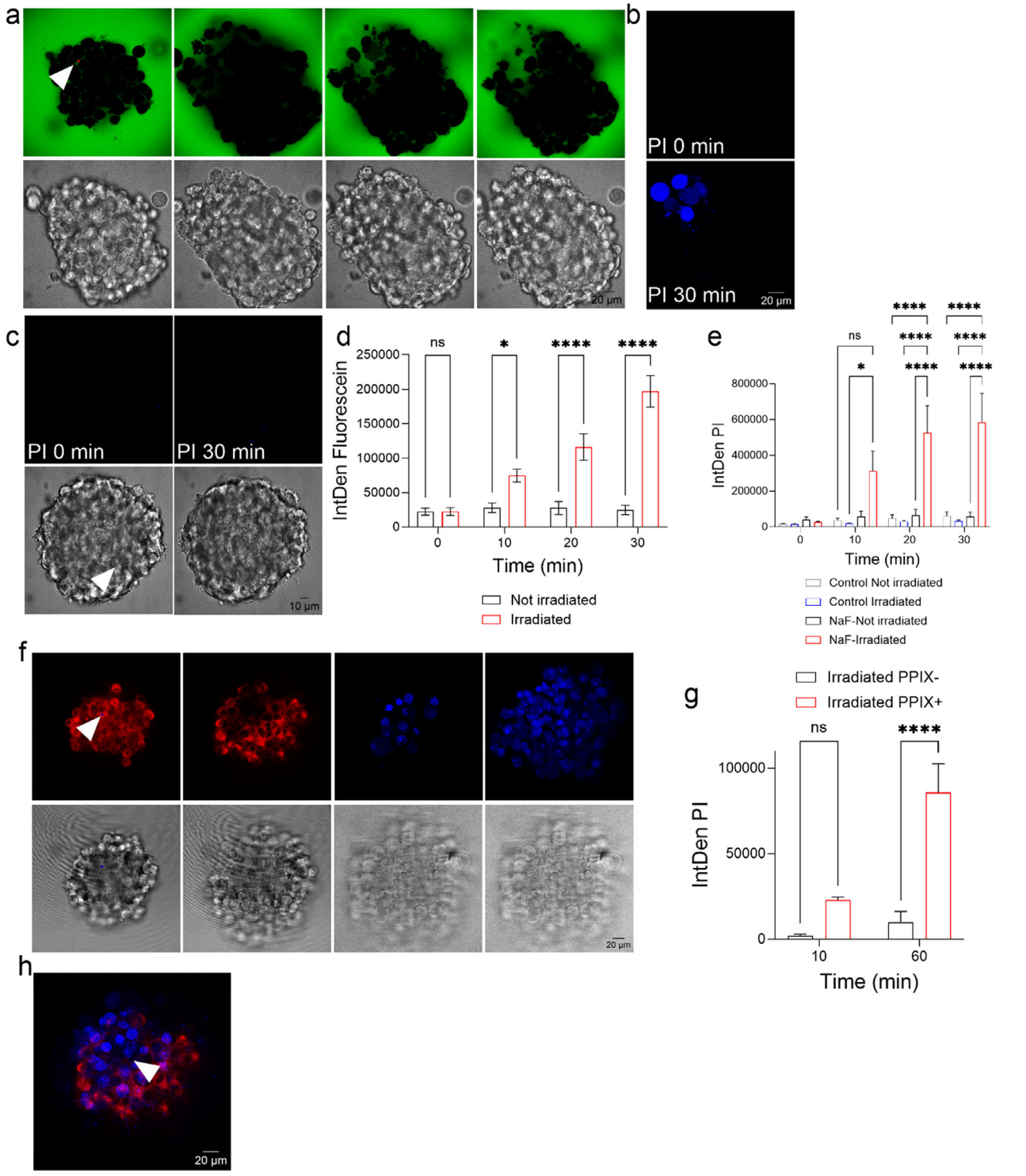

Figure 5. Fluorescein and protoporphyrin localization after laser bleaching in U87 spheroids. a) Representative confocal images of fluorescein (upper panel) and bright field image (lower panel) of a U87 spheroid treated with fluorescein before bleaching (left panel), after bleaching (central left panel),10 min after laser bleaching (central right panel) and 30 min after laser bleaching (right panel). Scale bar is 20 µm. b) PI internalization. c) PI internalization in not NaF irradiated-treated spheroids. d) Quantitative NaF internalization (e) Quantitative NaF internalization. f) Representative confocal images of protoporphyrin (red-upper panel), propidium iodide (blue-upper panel) and bright field image (lower panel) of a U87 spheroid treated with 5-ALA without serum before bleaching (left panel), after bleaching (central left panel), 10 min (central right panel) and 1 h after laser bleaching (right panel). Scale bar is 20 µm. g) PI internalization quantification of irradiated PPIX spheroids versus control spheroids (no PPIX) (h) Representative confocal merge of protoporphyrin (after irradiation) and maximal z-projection of propidium iodide, corresponding to the spheroid represented in panel b, 10 min post laser irradiation. Scale bar is 20 µm.

spheroids. For this, the dyes needed to be localized within the spheroid structure. Interestingly, NaF, localized internally within the spheroids (and extracellularly), and that fluorescein concentration can be used to induce damage to the spheroids. This approach presents several advantages. First, irradiation is performed only inside the spheroid, generating no irradiation or damage to the surrounding normal tissue. Second, photo damage is induced at the center of the spheroid. This central damage disrupts the 3D structure of the spheroid and uptake of PI, as observed in Figure 5a–c. Regarding PPIX, damage can also be induced at the center of the spheroid, as PPIX is uniformly distributed. As shown in Figure 5e–g, cell death is induced only in the irradiated part of the spheroid, leaving the other parts intact. This again corroborates the cell death selectivity of this technique.

5. Conclusion

To the best of our knowledge, PDT using single-point laser irradiation has not been explored. Here, we have presented a new photodynamic therapy mechanism through the combination of clinical fluorescent markers and focused laser technology. This necrotic cell death is induced by compromising the plasma membrane in a precise and selective manner in 2D glioblastoma cancer cells. The method was also tested in a spheroid model, where it enabled cell death induction at the center of the spheroids. Future steps to improve SPL-PDT include changes in the organelle target or the use of two-photon microscopy, where fluorescent markers can be activated at the laser focus, further enhancing the selectivity of cell death.

Supporting Information

Supporting Information is available from the Wiley Online Library or from the author.

Acknowledgements

This work was financed by the AECC (Spanish Association Against Cancer) IDEAS21989THOM and Ministerio de Ciencia e Innovación: CNS2024-154353. C.S.C. Thanks to the Comunidad Autónoma Madrid for the Ayudante de investigación contract number 45576. We acknowledge financial support from the Spanish State Research Agency, AEI/10.13039/501100011033, through the "Severo Ochoa" Programme for Centres of Excellence in R&D: CEX2023-001386-S.

Conflict of Interest

The authors declare no conflict of interest.

Data Availability Statement

The data that support the findings of this study are available from the corresponding author upon reasonable request.

Keywords

fluorescein, laser, necrosis, photodynamic Therapy, plasma Membrane, protoporphyrin IX, spheroids

Received: December 7, 2024
Revised: June 19, 2025
Published online:

[1] J. H. Correia, J. A. Rodrigues, S. Pimenta, T. Dong, Z. Yang, *Pharmaceutics* **2021**, *13*, 1332.
[2] D. Bhanja, H. Wilding, A. Baroz, M. Trifoi, G. Shenoy, B. Slagle-Webb, D. Hayes, Y. Soudagar, J. Connor, A. Mansouri, *Cancers (Basel)* **2023**, *15*, 3427.
[3] S. Ebrahimi, M. Khaleghi, W. Stummer, A. Gorji, *Life Sci.* **2024**, *351*, 122808.
[4] S. Singh, A. Aggarwal, S. Thompson, J. P. C. Tomé, X. Zhu, D. Samaroo, M. Vinodu, R. Gao, C. M. Drain, *Bioconjug. Chem.* **2010**, *21*, 2136.
[5] S. A. Thompson, A. Aggarwal, S. Singh, A. P. Adam, J. P. C. Tome, C. M. Drain, *Bioorganic Med. Chem.* **2018**, *26*, 5224.
[6] H. Cheng, P. Yuan, G. Fan, L. Zhao, R. Zheng, B. Yang, X. Qiu, X. Yu, S. Li, X. Zhang, *Appl. Mater Today* **2019**, *16*, 120.
[7] S. Thompson, X. Chen, L. Hui, A. Toschi, D. a Foster, C. M. Drain, *Photochem. Photobiol. Sci.* **2008**, *7*, 1415.
[8] J. F. Algorri, M. Ochoa, P. Roldán-Varona, L. Rodríguez-Cobo, J. M. López-Higuera, *Cancers (Basel)* **2021**, *13*, 3484.
[9] P. S. Maharjan, H. K. Bhattarai, *J. Oncol.* **2022**, *2022*, 7211485.
[10] J. Kim, O. A. Santos, J. H. Park, *J. Controlled Release* **2014**, *191*, 98.
[11] K. Nakajima, H. Takakura, Y. Shimizu, M. Ogawa, *Cancer Sci.* **2018**, *109*, 2889.
[12] L. Cramer Ahrens, M. Green Krabbenhøft, R. Würgler Hansen, N. Mikic, C. B. Pedersen, F. R. Poulsen, A. R. Korshoej, *Cancers (Basel)* **2022**, *14*, 1.
[13] S. Schipmann, M. Schwake, E. Suero Molina, W. Stummer, *J. Neurol. Surgery, Part A Cent. Eur. Neurosurg.* **2019**, *80*, 475.
[14] L. M. Wang, M. A. Banu, P. Canoll, J. N. Bruce, *Front. Oncol.* **2021**, *11*, 1.
[15] B. Musca, C. Bonaudo, A. Tushe, G. Battaggia, M. G. Russo, M. Silic-Benussi, A. Pedone, A. Della Puppa, S. Mandruzzato, *J. Neurosurg.* **2024**, *140*, 958.
[16] X. Cheng, J. Chen, R. Tang, J. Ruan, D. Mao, H. Yang, *Cancers (Basel)* **2023**, *15*, 1.
[17] P. A. Sutton, M. A. Van Dam, R. A. Cahill, S. Mieog, K. Polom, A. L. Vahrmeijer, *BJS Open* **2023**, *7*, 1.
[18] J. T. Senders, I. S. Muskens, R. Schnoor, A. V. Karhade, *Acta Neurochir. (Wien).* **2017**, *159*, 151.
[19] R. Sun, H. Cuthbert, C. Watts, *Cancers (Basel)* **2021**, *13*, 3508.
[20] A. J. Schupper, M. Rao, N. Mohammadi, R. Baron, J. Y. K. Lee, F. Acerbi, C. G. Hadjipanayis, *Front. Neurol.* **2021**, *12*, 682151.
[21] L. C. Crowley, A. P. Scott, B. J. Marfell, J. A. Boughaba, G. Chojnowski, N. J. Waterhouse, *Cold Spring Harb. Protoc.* **2016**, *2016*, 647.
[22] F. Perche, V. P. Torchilin, *Cancer Biol Ther* **2012**, *13*, 1205.
[23] T. Ogino, H. Kobuchi, K. Munetomo, H. Fujita, M. Yamamoto, T. Utsumi, K. Inoue, T. Shuin, J. Sasaki, M. Inoue, K. Utsumi, *Mol. Cell. Biochem.* **2011**, *358*, 297.